2007-4 Working Paper

Characterizing and modeling preferential flow using magnetic resonance imaging and multifractal theory

Adolfo Posadas, International Potato Center (CIP), and Universidad Nacional Mayor de San Marcos, FCF-DAFI, Lima, Peru,
Roberto Quiroz, International Potato Center (CIP), Lima, Peru
Silvio Crestana, CNPDIA/EMBRAPA, São Carlos, SP, Brazil
Roberto N. Onody, IFSC – USP, São Carlos, SP, Brazil
Alberto Tanus, IFSC – USP, São Carlos, SP, Brazil
Carlos H. Panepucci, IFSC – USP, São Carlos, SP, Brazil

ISBN 978-92-9060-326-9
Natural Resources Management Division
Working Paper
No. 2007-4

Table of Contents

Abstract

The study of water movement in soils is of fundamental importance in hydrologic science. It is generally accepted that in most soils, water and solutes flow through unsaturated zones via preferential paths. This paper combines magnetic resonance imaging (MRI) with multifractal theory and the invasion percolation model (IPMod) in order to characterize and simulate preferential flow. A cubic double-layer column filled with fine and coarse texture sand was placed into a MRI system. Water infiltration through the column was recorded in both dynamic and steady state conditions. Twelve sections were obtained and characterized using multifractal theory. An algorithm code for a 3-D model, based on the IPMod, was developed and validated with the MRI images. The MRI system provided a detailed description of the preferential flow under steady state conditions and was also useful in understanding the dynamics of the formation of the fingers. The calculated fractal dimension was not adequate for making an inference about the spatial distribution of water along the column profile. The $f(\alpha)$-α spectrum was very sensitive to the variation encountered at each coronal slice of the column providing a suitable characterization of the dynamics of the process. 3-D modeling with the improved IPMod produced images similar to the ones obtained with MRI. In conclusion, MRI could adequately characterize preferential flow, and the fingering process was adequately simulated by combining multifractal analysis with 3-D modeling techniques.

Abbreviations: MRI, magnetic resonance image; IPM, invasion percolation model

Acknowledgements

This work was supported by EMBRAPA; Instituto de Física de São Carlos, Universidad de São Paulo, Brazil; The Ecoregional Fund; and CIP's Natural Resources Management Division.

Dr. Carlos H. Panepucci passed away in 2006 without being able to participate in the preparation of this paper. We gratefully acknowledge his active and valuable contributions throughout the duration of this project.

Characterizing and modeling preferential flow using magnetic resonance imaging and multifractal theory

INTRODUCTION

Fluid flow through preferential paths, or fingers, is extremely important in agricultural processes such as infiltration of water and transport of agrochemicals through the soil profile. The role that the preferential flow plays is of particular interest in the transport of pesticides, heavy metals, radioactive waste and other contaminants. The probability of contaminating ground water and therefore compromising the quality of water resources increases with the existence of preferential paths.

In order to understand this extremely complex problem, some researchers concentrate their efforts on studying fluid transport in connection with the geometry of porous media (Lu et al., 1994). Many experiments have shown that fluid transport-porous medium coupling has auto-similarity or fractal characteristics in a range of defined scales (Katz and Thompson, 1985). The fingering phenomenon in soils, which is basically of capillary character, also presents fractal characteristics (Chang et al., 1994; Posadas and Crestana, 1993). These fractal characteristics have led to the creation of simulation models such as the Diffusion Limited Aggregation-DLA (Chen and Wilkinson, 1985) that simulates the viscous fingering phenomenon and the invasion percolation model (Wilkinson and Willemsen, 1983), which in turn simulates the capillary fingering phenomenon.

Recently, Steenhuis and Parlange (1996) have published a review of the principal theories of the fingering phenomena, both in the laboratory and in the field. In this review, a model using a modification of the invasion percolation model was introduced (Glass and Yarrington, 1996). Other researchers have confirmed the suitability of fractal and multifractal theory to describe and simulate preferential flow, as shown in the few examples that follow. Ogawa et al. (2002) used fractal analysis to study preferential flow in field soils. They evidenced a good correlation between the surface fractal dimension and the exponent of a Van Genuchten expression applied to the particle size distribution of the soil. A multifractal analysis was successfully employed by Nittmann et al. (1987) and Måløy et al. (1987) on viscous fingering structures observed in Hele-Shaw cells and in a mono-layer of glass beads, respectively. Recent literature suggests that the multifractal formalism is applicable to three-dimensional systems, for example, Held and

Illangasekare (1995) showed that the width (internal energy or $\Delta\alpha$) of the $f(\alpha)$ curve (multifractal spectrum), in the range of positive moments, quantifies displacement instability.

This paper proposes an innovation in the characterization of preferential flow by combining MRI (Posadas et al., 1996; Crestana and Posadas, 1997) with multifractal theory (Chhabra et al., 1989, Posadas et al., 2001, 2003) for a three dimensional description of the dynamic of fingers in sandy soils. The results were also used to extend the modified invasion percolation model as described by Onody et al. (1995), to simulate the morphology of the fingers in three dimensions.

MATERIALS AND METHODS

Experiment

In order to visualize, characterize and simulate the fingering phenomenon in three dimensions, magnetic resonance imaging (MRI) technique (CNPDIA/EMBRAPA Laboratory, Brazil), multifractal theory and a modified invasion percolation model were employed, both in dynamic and in static conditions (Posadas, 1994; Onody et al., 1995; Posadas et al., 1996). A cubic 15x15x15 cm double-layer sand column was built. The top layer was 2.5 cm high, consisting of fine texture soil sand (particle size diameter in mm: , $0.106 < d < 0.149$ porosity in %, $\phi = 44.8$, saturated hydraulic conductivity in cm/s: $K_s = 6.3x10^{-3}$ and bulk density in g/cm^3: $\rho_b = 1.6$) and the lower 12.0 cm layer was filled with coarse sand (particle size diameter in mm: $0.212 < d < 0.500$, porosity in %, $\phi = 31.2$, saturated hydraulic conductivity in cm/s: $K_s = 26.7x10^{-3}$ and bulk density in g/cm^3: $\rho_b = 1.6$). On the surface of the top layer, an acrylic plate of 15x15x0.3 cm with 1.0 mm diameter holes was placed, in order to spread water uniformly over the surface. The top 0.2 cm section of the column remained free for water application. This column was placed into the head coils of the 500 Gauss MRI systems (Figure 1). The infiltration of water through the cubic column was studied under hydrodynamic steady state conditions. It was also possible to follow the spatial dynamics of the wetting front by means of a MRI system measuring the spin echo signal (Posadas et al., 1996).

a)

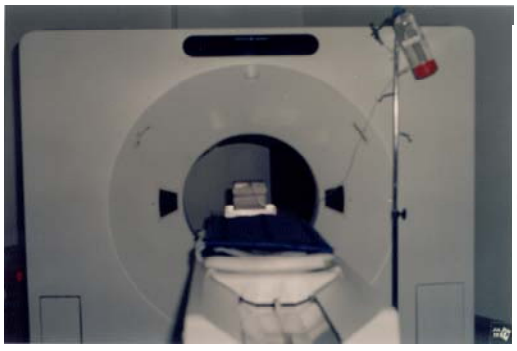

b)

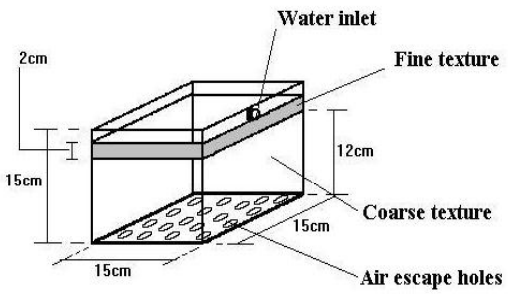

Fig. 1.
a) 500 Gauss MRI system (IFSC-USP Laboratory, Brazil) showing the cubic column used
b) Sketch of the cubic column.

THEORY

Multifractal

It is now widely accepted that physical systems that exhibit chaotic behavior are generic in nature. Since these systems lose information exponentially fast it is possible to follow and predict their motion in any detail only for short time scales (Chhabra et al., 1989). To describe their long-term dynamical behavior, one must resort to suitable statistical descriptions. One such description is multifractal formalism (Chhabra, et al., 1989; Hentschel and Procaccia, 1983; Halsey et al., 1986; Chhabra and Jensen, 1989). Multifractal theory permits the characterization of complex phenomena in a fully quantitative fashion, for both temporal and spatial variations. Multifractal techniques and notions are increasingly widely recognized as the most appropriate and straightforward framework within which to analyze and simulate not only the scale dependency of the geophysical observables, but also their extreme variability over a wide range of scales (Schertzer and Lovejoy, 1994).

The basic equation of fractal theory expresses the relationship between the number and the size of the objects (Feder, 1988):

$$N(\varepsilon) \sim \varepsilon^{-D_0}, \qquad [1]$$

where $N(\varepsilon)$ is the number of objects, ε is the scale and D_0 is the fractal dimension. The box-counting technique is used to estimate the scaling properties of a set by covering the set with boxes of size ε and counting the number of boxes containing at least one pixel representing the object under study:

$$D_0 = -\lim_{\varepsilon \to 0} \frac{LogN(\varepsilon)}{Log(\varepsilon)}. \qquad [2]$$

Provided the limit exists, the infinitum of N(ε) is approximated by varying the origin of the grid until the smallest number is found. Using equation [2], the box-counting dimension D0 can be determined as the negative slope of log N(ε) versus log(ε), measured over a range of box widths.
In a homogeneous system, the probability (P) of a measured quantity (measure) varies with scale ε as (Chhabra et al., 1989; Evertsz and Mandelbrot, 1992, and Vicsek, 1992):

$$P(\varepsilon) \sim \varepsilon^{D}, \quad [3]$$

where D is a fractal dimension. For heterogeneous or non-uniform systems the probability within the i-th region Pi varies as:

$$P_i(\varepsilon) \sim \varepsilon^{\alpha_i}, \quad [4]$$

where αi is the Lipschitz-Hölder exponent or singularity strength, characterizing scaling in the i-th region or spatial location (Feder, 1988). The parameter αi quantifies the degree of regularity in point x i. Loosely speaking, any measure μ of an interval [x i, x i +Δx], behaves as (Δx)αi (Halsey et al., 1986). For a uniform distribution one finds αi (x) = 1 for all x. More generally, for any real value a > 0 the distribution with density xa-1 on [0,1] has αi(0) = a and αi(x) = 1 for all x$\in$ [0,1]. Values αi(x) < 1 indicate, thus, a burst of the event around x "on all levels", while αi(x) > 1 is found in regions where events occur sparsely (Riedi, 1999). Similar αi values might be found at different positions in the space. The number of boxes N(α) where the probability Pi has singularity strengths between α and α+dα is found to scale as (Chhabra et al., 1989; Halsey et al., 1986):

$$N(\alpha) \sim \varepsilon^{-f(\alpha)}, \quad [5]$$

where f(α) can be considered as the generalized fractal dimension of the set of boxes with singularities α (Kohmoto, 1988). The exponent α can take on values from the interval [α-∞,α+∞], and f(α) is usually a function with a single maximum at df(α(q))/dα(q) = 0 (where q is the order moment of a statistic distribution). Thus, when q = 0, fmax is equal to the box-counting dimension, D0 (Gouyet, 1996; Vicsek, 1992).

Multifractal sets can also be characterized on the basis of the generalized dimensions of the q-th order moment of a distribution, Dq, defined as (Hentschel and Procaccia, 1983):

$$D_q = \lim_{\varepsilon \to 0} \left(\frac{1}{q-1} \quad \frac{\log \mu(q,\varepsilon)}{\log(\varepsilon)} \right), \qquad [6]$$

where $\mu(q, \varepsilon)$ is the partition function (Chhabra et al., 1989):

$$\mu(q,\varepsilon) = \sum_{i=1}^{N(\varepsilon)} P_i^q(\varepsilon). \qquad [7]$$

The generalized dimension Dq is a monotonic decreasing function for all real q's within the interval $[-\infty, +\infty]$. When $q < 0$, μ emphasizes regions in the distribution with less concentration of a measure, whereas the opposite is true for $q > 0$ (Chhabra and Jensen, 1989).

Also, the partition function scales as:

$$\mu(q,\varepsilon) \sim \varepsilon^{\tau(q)}, \qquad [8]$$

where $\tau(q)$ is the correlation exponent of the q-th order moment defined as (Halsey et al., 1986; Vicsek, 1992):

$$\tau(q) = (q-1)D_q. \qquad [9]$$

The connection between the power exponents *f(α)* (Equation [5]) and *τ(q)* (Equation [9]) is made via the Legendre transformation (Callen, 1985; Chhabra and Jensen, 1989; Halsey et al., 1986):

$$f(\alpha(q)) = q\alpha(q) - \tau(q)$$

and [10]

$$\alpha(q) = \frac{d\tau(q)}{dq} \quad .$$

f(α) is a concave downward function with a maximum at $q = 0$. When q takes the values of $q = 0$, *1* or *2,* equation [6] is reduced to:

$$D_0 = \lim_{\varepsilon \to 0} \frac{\log(N(\varepsilon))}{\log(\varepsilon)}, D_1 = \lim_{\varepsilon \to 0} \frac{\sum_{i=1}^{N(\varepsilon)} \mu_i(\varepsilon) \log(\mu_i(\varepsilon))}{\log(\varepsilon)}, \mathrm{D}_2 = \lim_{\varepsilon \to 0} \frac{\log(C(\varepsilon))}{\log(\varepsilon)}, \quad [11]$$

respectively, with C(ε) being the correlation function.

The values D0, D1 and D2 are known as the capacity dimension, the entropy dimension and the correlation dimension, respectively. The capacity dimension provides global (or average) information about a system (Voss, 1988). The entropy dimension is related to the information (or Shannon) entropy (Shannon and Weaver, 1949). The correlation dimension D2 is mathematically associated with the correlation function (Grassberger and Procaccia, 1983) and computes the correlation of measures contained in a box of size ε. The relationship between

D_0, D_1, and D_2 is,

$$\mathrm{D}_2 \leq \mathrm{D}_1 \leq \mathrm{D}_0, \quad [12]$$

where the equality D0 = D1 = D2 occurs only if the fractal is statistically or exactly self-similar and homogeneous (Korvin, 1992).

Following the methodology used in Posadas et al. (2001, 2003), multifractal theory was applied to the MR images of the fingering phenomena. Twelve slices of coronal sections, following the gravitational force, were analyzed using the multifractal analysis and scaling system algorithm (MASS –downloadable after subscription at http://inrm.cip.cgiar.org/vlab)

Invasion Percolation

Onody et al. (1995) developed the 2-D site invasion percolation model to simulate the fingering phenomena. The model uses four parameters: G_1: hydraulic pressure, G_2: proportional to the numbers of fingers, G_3: surface tension, and G_4: proportional to the wet area of the experiment. The authors showed that with these four parameters the fingering phenomenon in 2-D events could be successfully simulated for three types of soils with different textures.

To extend the 2-D model of the physical processes of the fingering phenomenon to a 3-D representation, certain similarities were assumed. In both cases, hydraulic pressure and gravity force constitute the main forces producing a downward movement. The 3-D model conserved all

four G parameters describing the 2-D model. The only difference was that the parameters G_3 and G_4 had spatial components (x, y, z). The 3-D model was tested using the same soil types reported by Onody et al. (1995), with the following input values: G_1=-0.020, G_2=0.75, G_3=0.35, and G_4=0.15.

RESULTS AND DISCUSSION

The results obtained with the MRI system are depicted in Figures 2 and 3. Figure 2 shows three acquisitions of the transverse plane of the cubic sand column at steady-state flow. In these three images it is possible to observe the three-dimensional character of the fingering phenomena and its spatial variability. The accumulation of water at the bottom of the column can be seen in panel A. Since there is no evidence of water flow except through preferential paths it can be inferred that, if the experiments replicate the process occurring in real systems, the movement of water and the solutes conveyed within it could reach shallow or deep water pools in the soil faster than in conditions where preferential flow is absent.

The column under steady-state flow was "dissected" into 12 horizontal (coronal) slices of 1.0 cm thick, as shown in Figure 3. In the figure, the gray scale depicts the concentration of water in the cross section. It can be seen that the water concentration throughout the profile follows a fixed path. Areas outside this fixed path remained dry. These findings support the existence of preferential flow under the conditions studied (Posadas et al., 1996).

The dynamic of the fingering process is evidenced in the graphics shown in Figure 4. Panel A evidences that the first finger advanced nearly half way through the column, some 36 s after the onset of the run whereas a second finger is just being initiated. At the end of the run, after 137 s (Panel C), two fingers are clearly formed and constitute the only means by which the water reaches the bottom of the column. It can thus be stated that water movement in sandy soils presents spatial and temporal variability that must be understood in order to adequately simulate the process.

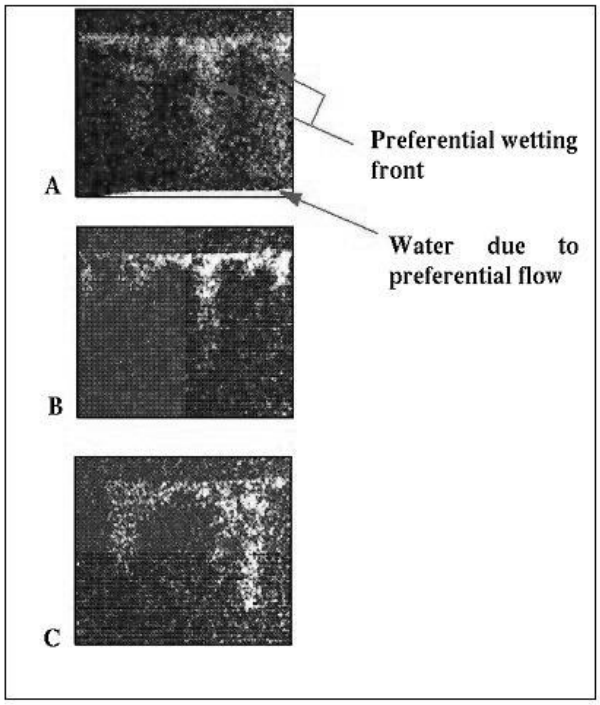

Fig. 2. Images obtained by MRI showing twelve coronal sections (slices 1.0 mm thick) of the cubic soil column following the direction of the infiltration.

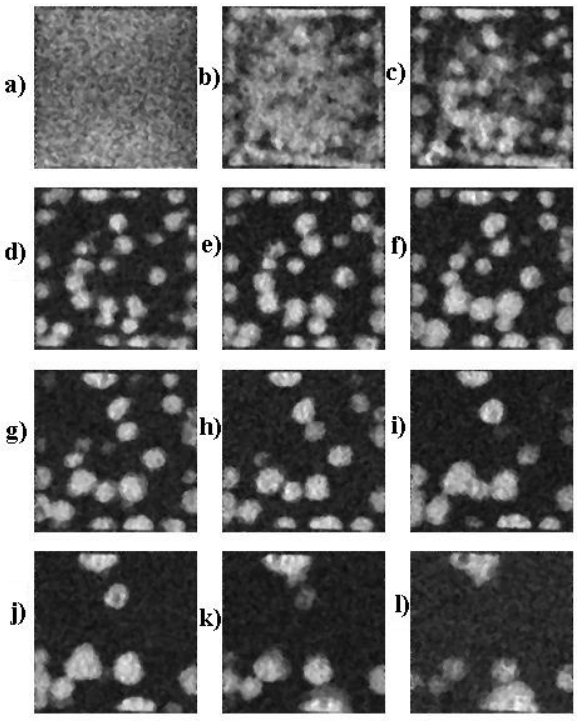

Fig. 3. **a)** Saturated section near the surface of the column (first layer), **l)** section corresponding to the bottom of the soil column; and **b)** through **k)** represent intermediate situations. Gray levels represent water content.

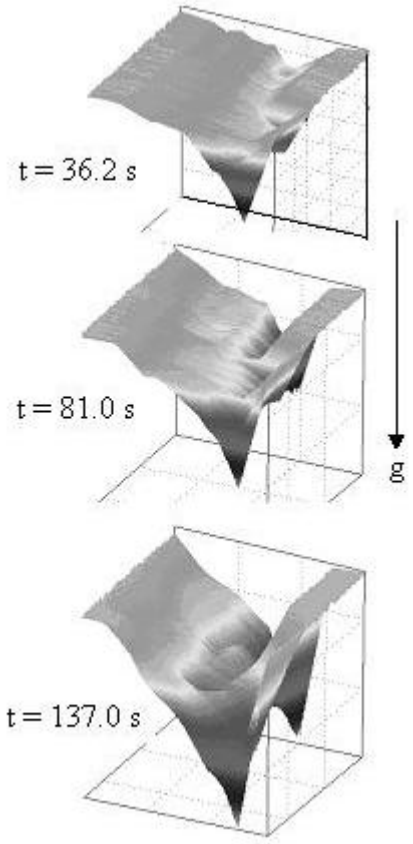

Fig. 4.
Wetting front along the cubic column through time. The panels show the spatial distribution of fluid displacement profile front, following gravity; t = 36.2, 81.0 and 137.0 (end) seconds.

Figures 5, 6, and 7 summarize the fractal analysis. The capacity or fractal dimension (D0, Figure 5) evidences differences in the spatial distribution among the twelve layers of the columns depicted in Figure 3. The top layer in the system seems to be more heterogeneous and the heterogeneity of the distribution of water is reducing towards the bottom of the column. This seems to be a good descriptor of the steady state conditions at which the images were taken.

A multifractal analysis was also used to describe the heterogeneity of the spatial variability of the water in each cross section throughout the profile of the column (Figure 6). A quick inspection along the column indicates how dynamic the system is, even though the analysis was made when the system reached a steady-state flow. It goes from the wetting instability—the first condition of the coarse texture substrate (Panel B in Figure 3)—to a hydrodynamic stability at the

bottom (Panel L in Figure 3), passing though chaotic sections in the intermediate portion (Panels C through K in Figure 3).

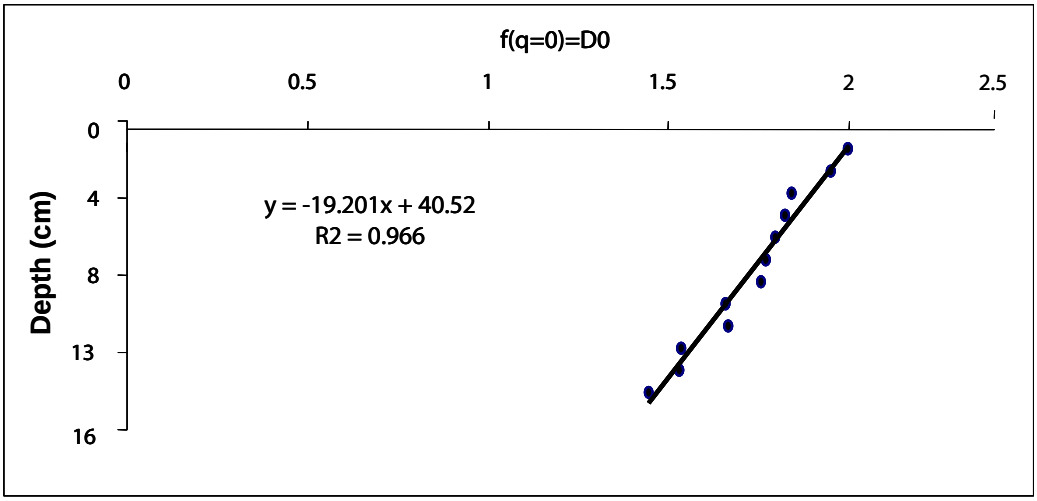

Fig. 5. Fractal dimension, of the fingers, measured along the vertical depth.

The spatial variations in all these conditions seem to be well characterized with the f(α)-α spectrum shown on the right panels in Figure 6. For instance, the cross section labeled MRI11 represents the wetting instability conditions in the column. This hydrodynamic instability is attributed to the change produced when the water flows from the fine to the coarse texture. The multifractal spectrum is characteristic of a heterogeneous system with variations on both sides of the maximum value. From the maximal fractal dimension (D0) to the left, the spectrum describes the behavior of the areas where water is present (positive q's). The asymmetry toward the right from α=2 indicates domination of small or extremely small values of water. This is an indication of the existence of preference paths. The condition prevails, with small variations, down to the sixth coronal section (half way through the column along the gravitational force). Inspection of the variation in internal energy ($\Delta\alpha$) shows that the $\Delta\alpha$ value for MRI11 is 1.36. Compared to the near-saturation condition presented in the layer with fine texture ($\Delta\alpha$=0.21) one can contrast how this multifractal parameter changes when the condition changes from a quasi-homogeneous (MRI12) to a heterogeneous wetting instability. The coronal section labeled MRI05 seems to represent the zone within the column where the transition from instability to hydrodynamic stability initiates. The corresponding $\Delta\alpha$ is around 0.3. The bottom three coronal sections correspond to hydrodynamic stability, behaving as a pure fractal with a $\Delta\alpha < 0.07$.

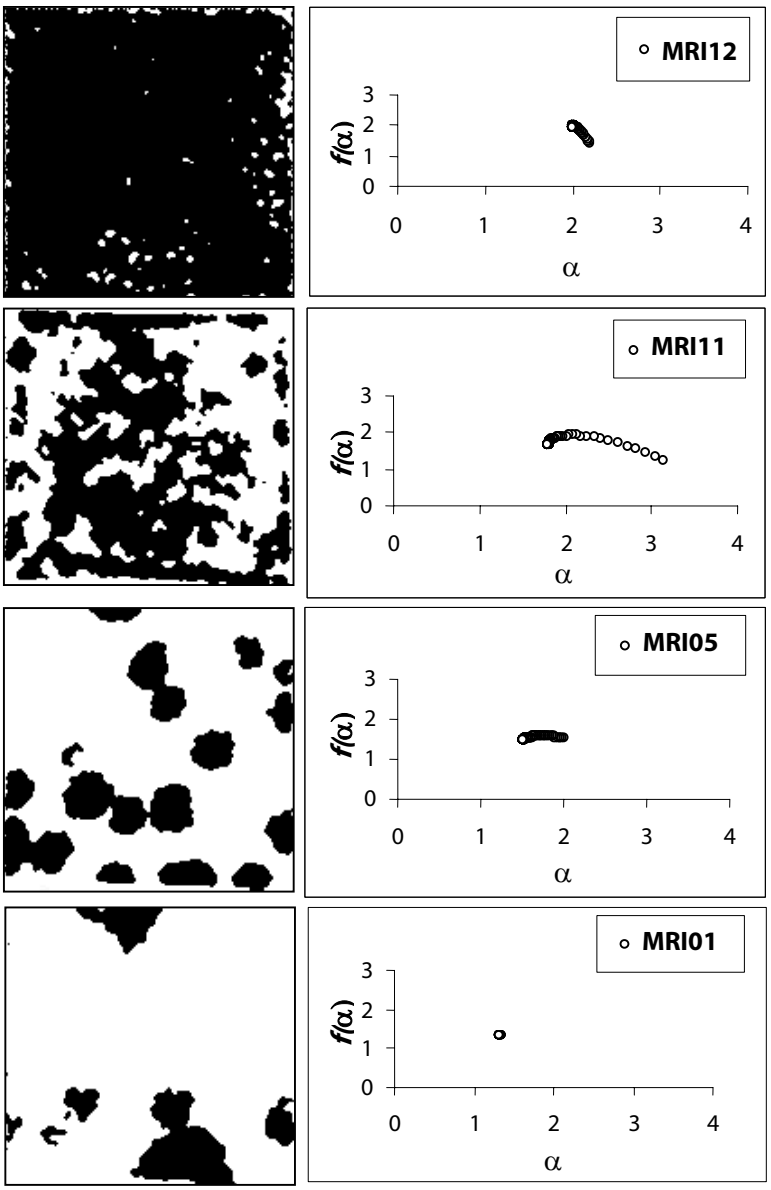

Fig. 6.
Magnetic Resonance Images from a three-dimensional fingering phenomena and multifractal spectrums following the gravitational direction (from top MRI12 to bottom MRI01).

An interesting feature of the multifractal analysis is that in spite of the fact that the image was taken under steady-state flow, the dynamic characteristic present in the profile can be described by the f(α)-α spectrum and its parameters. As an example, Figure 7 shows how the changes in one of the multifractal parameters, associated with the internal energy ($\Delta\alpha$), seems to describe the dynamics of water along the column depth. Three stages are clearly evidenced in this figure, the instability zone, the transition zone, and the equilibrium zone or the depth at which

hydrodynamical stability has been achieved. This variation could not be addressed if the conventional fractal analysis (using the capacity dimension only) is used, as shown above (Figure 5).

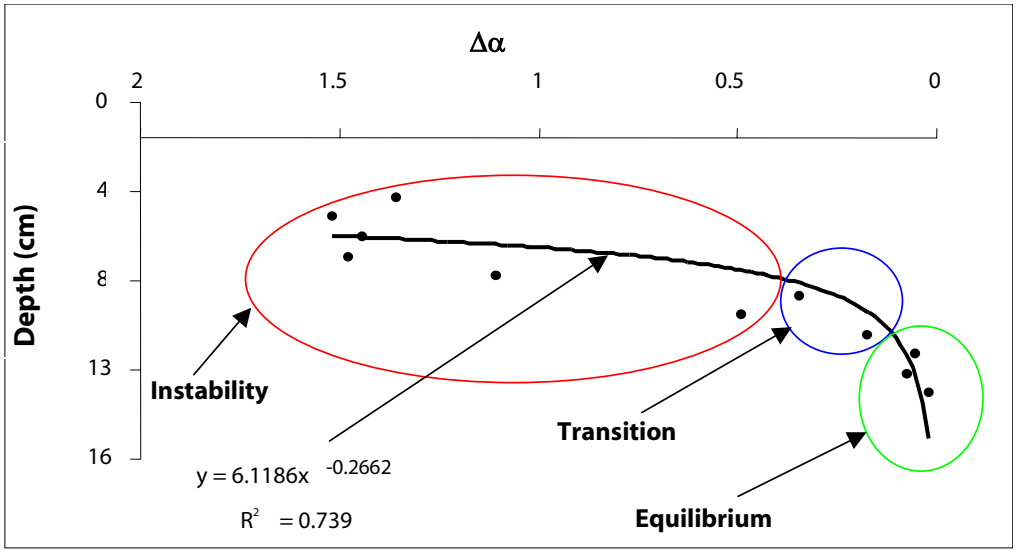

Fig. 7. Variation of internal energy of the system as a function of depth along the cubic column.

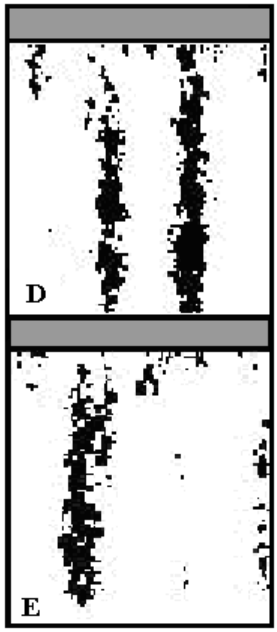

Fig. 8. Traversal sections showing the simulated fingering phenomena using the extended 3-D invasion percolation model.

The simulation results, using the 3-D extended model from Onody et al. (1995) are shown in Figure 8. Panels A and B show different transversal sections of the simulated column. The similarity between observed and simulated fingers evidence the capability of the 3-D model to

depict preferential flow process in sandy soils. This tool could become useful in hydrology and environmental studies where preferential flow plays an important role.

CONCLUSIONS

Both the percolation model and the MRI system were shown to be good tools to characterize and simulate preferential flow in soils. The MRI system is useful in visualizing the phenomenon for a better understanding of the process. However, very few research groups have access to this type of equipment. The 3-D invasion percolation model combined with the use of multifractal theory could facilitate the study of the dynamics of preferential flow and can be used to predict outcomes under real conditions. The combination of these techniques open a new set of alternatives that must be further tested for different soil types and management conditions.

REFERENCES

Callen, H.B. 1985. *Thermodynamics and an Introduction to Thermostatics.* 2d. ed. New York: John Wiley & Sons.

Chang, W-L, J.W. Biggar, and D.R. Nielsen. 1994. Fractal description of wetting front instability in layered soils. *Water Resources Research* 30(1): 125-132.

Chen, J.D. and D. Wilkinson. 1985. Pore-scale viscous fingering in porous media. *Physical Review Letters* 58(18): 1892-1895.

Chhabra, A.B., and R.V. Jensen. 1989. Direct determination of the f(α) singularity spectrum. *Physical Review Letters* 62: 1327-1330.

Chhabra, A.B., C. Meneveu, R.V. Jensen, and K.R. Sreenevasan. 1989. Direct determination of the f(α) singularity spectrum and its application to fully developed turbulence. *Physical review. A, General physics, 3rd Series* 40: 5284-5294.

Crestana, S. and D.A.N. Posadas. 1998. 2-D and 3-D fingering phenomenon in unsaturated soils investigated by fractal analysis, invasion percolation modeling and non-destructive image processing. In *Fractals in Soil Science*, ed. P. Baveye, J.Y. Parlange and B.A. Stewart, 293-332. Boca Raton: CRC Press.

Evertsz, C.J.G. and B.B. Mandelbrot. 1992. Multifractal measures. In *Chaos and Fractals. New Frontiers of Science*, ed. H.-O. Peitgen, H. Jurgens, and D. Saupe, 921-953. New York: Springer-Verlag.

Feder, J. 1988. *Fractals.* New York: Plenum Press.

Glass, R.J. and L. Yarrington. 1996. Simulation of gravity fingering in porous media using a modified invasion percolation model. *Geoderma* 70(2-4): 231-252.

Gouyet, J.F. 1996. *Physics and Fractals Structure.* (New York: Springer).

Grassberger, P. and I. Procaccia. 1983. Characterization of strange attractors. *Physical Review Letters* 50(5): 346-349.

Halsey, T.C., M.H. Jensen, L.P. Kadanoff, I. Procaccia, and B.I. Shraiman. 1986. Fractal measures and their singularities of strange sets. *Physical Review A* 33(2): 1141-1151.

Held, R.J. and T.H. Illangasekare. 1995. Fingering of dense nonaqueous phase liquids in porous media. 2. Analysis and classification. *Water Resources Research* 31(5): 1223-1231.

Hentschel, H.G.E., and I. Procaccia. 1983. The infinite number of generalized dimensions of fractals and strange attractor. *Physica D* 8(3): 435-444.

Katz, A.J. and A.H. Thompson. 1985. Fractal sandstone pores: implications for conductivity and pore formation. *Physical Review Letters* 54(12): 1325-1328.

Kohmoto, M. 1988. Entropy function for multifractals. *Physical review A.* 37(4): 1345-1350.

Korvin, G. 1992. Fractals models. In *The Earth Sciences*. Elsevier, Amsterdam, The Netherlands.

Lu, T.X., J.W. Biggar and D.R. Nielsen. 1994. Water movement in glass bead porous media, 2. Experiments of infiltration and finger flow. *Water Resource Research* 30(12): 3283-3290.

Mandelbrot, B.B. 1982. *The fractal geometry of nature*. 2d ed. N.Y.: W.H. Freeman and Company. p. 480.

Måløy, K. J., F. Boger, J. Feder, and T. Jøssang. 1987. Dynamics and structure of viscous fingering in porous media. In *Time-Dependent effects in disordered materials, ed.* R. Pynn and T. Riste, 111-118. N.Y.: Plenum Press.

Nittmann, J., H. E. Stanley, E. Toubul, and G. Daccord. 1987. Experimental evidence of multifractality. *Physical Review Letters* 58(6): 619-622.

Ogawa, S., P. Baveye, J-Y. Parlange, and T. Steenhuis. 2002. Preferential flow in the field soils. *Forma* 17(1): 31-53.

Onody, R.N., D.A.N. Posadas, and S. Crestana. 1995. Experimental studies of fingering phenomena in two dimensions and simulation using a modified invasion percolation. *Journal of Applied Physics* 78(5): 2970-2976.

Posadas, A.N.D., D. Gimenez, M. Bittelli, C.M.P. Vaz, and M. Flury. 2001. Multifractal Characterization of soil particle-size distribution. *Soil Science Society of America Journal* 65(5): 1361-1367.

Posadas, A.N.D., D. Gimenez, M. R. Quiroz and R. Protz. 2003. Multifractal Characterization of Soil Pore Systems. *Soil Science Society of America Journal* 67(5): 1361-1369.

Posadas, A.N.D. 1994. Estudo do fenômeno "fingering" em um meio poroso através de imagens e teoria da percolação por invasão. PhD thesis. IFSC/USP. São Carlos- SP-Brazil.

Posadas, A.N.D., and S. Crestana. 1993. Aplicação da teoria fractal na caracterização do fenômeno "fingering" em solos. *Revista brasileira de ciencia do solo* 17(1): 1-8.

Posadas, A.N.D., A. Tannús, C.H. Panepucci, and S. Crestana. 1996. Magnetic resonance imaging as a non-invasive technique for investigating 3-D preferential flow occurring within stratified soil samples. *Computers and Electronics in Agriculture* 14(4): 255-267.

Riedi, R. 1999. Multifractals: An Introduction: Research report, Rice University 1997 (Version 5 September 1999). http:/www.dsp.rice.edu/~riedi.

Schertzer, D., S. Lovejoy. 1994. EGS Richardson AGU Chapman NVAG3 conference: Nonlinear Variability in Geophysics: scaling and multifractal processes. *Nonlinear Processes in Geophysics* 1: 77-79.

Shannon, C.E. and W. Weaver. 1949. *The Mathematical Theory of Communication.* Urbana, IL.: University of Illinois Press

Steenhuis, T.S. and J.Y. Parlange. 1996. A review of fingering phenomena. *Geoderma* 70.

Vicsek, T. 1992. *Fractal growth phenomena.* 2d ed. Singapore: World Scientific Publishing Co.

Voss, R.F. 1988. Fractals in nature: from characterization to simulation. In *The Science of Fractal Image*, ed. H.-O. Peitgen and D. Saupe, 21-69. New York: Springer.

Wilkinson, D. and J.F. Willemsen. 1983. Invasion percolation: a new form of percolation theory. *Journal of Physics A: Mathematical and General* 16: 3365-3376.

CIP's Mission

The International Potato Center (CIP) seeks to reduce poverty and achieve food security on a sustained basis in developing countries through scientific research and related activities on potato, sweetpotato, and other root and tuber crops, and on the improved management of natural resources in potato and sweetpotato-based systems.

The CIP Vision

The International Potato Center (CIP) will contribute to reducing poverty and hunger; improving human health; developing resilient, sustainable rural and urban livelihood systems; and improving access to the benefits of new and appropriate knowledge and technologies. CIP will address these challenges by convening and conducting research and supporting partnerships on root and tuber crops and on natural resources management in mountain systems and other less-favored areas where CIP can contribute to the achievement of healthy and sustainable human development.
www.cipotato.org

CIP is supported by a group of governments, private foundations, and international and regional organizations known as the Consultative Group on International Agricultural Research (CGIAR).
www.cgiar.org

International Potato Center
Apartado 1558 Lima 12, Perú • Tel 51 1 349 6017 • Fax 51 1 349 5326 • email cip@cgiar.org